Article:

eprints@whiterose.ac.uk
https://eprints.whiterose.ac.uk/

ARTICLE   OPEN

Check for updates

Applying laboratory methods for durability assessment of vitrified material to archaeological samples

Lorena Nava-Farias[1], James J. Neeway [1][✉], Michael J. Schweiger[2], José Marcial[1], Nathan L. Canfield[1], Carolyn I. Pearce [1], David K. Peeler[1], Edward P. Vicenzi [3], David S. Kosson[4], Rossane C. Delapp[4], John S. McCloy[5], Sam A. Walling [6], Clare L. Thorpe[6], Claire L. Corkhill [6], Russell J. Hand [6], Rolf Sjöblom[7] and Albert A. Kruger [2]

Laboratory testing used to assess the long-term chemical durability of nuclear waste forms may not be applicable to disposal because the accelerated conditions may not represent disposal conditions. To address this, we examine the corrosion of vitrified archeological materials excavated from the near surface of a ~1500-year old Iron Age Swedish hillfort, Broborg, as an analog for the disposal of vitrified nuclear waste. We compare characterized site samples with corrosion characteristics generated by standard laboratory durability test methods including the product consistency test (PCT), the vapor hydration test (VHT), and the EPA Method 1313 test. Results show that the surficial layer of the Broborg samples resulting from VHT displays some similarities to the morphology of the surficial layer formed over longer timescales in the environment. This work provides improved understanding of long-term glass corrosion behavior in terms of the thickness, morphology, and chemistry of the surficial features that are formed.

INTRODUCTION

Public acceptance is a critical part of the regulatory framework associated with the disposal of nuclear waste glass. Typically, to show that glass is chemically stable for long time periods and that the dominant corrosion mechanisms are well understood, waste glasses are subjected to short-term, accelerated laboratory tests. In addition, vitreous archaeological materials have long been considered as analogues that can be used to assess the corrosion behavior of nuclear waste glasses that will be disposed in subsurface geological repositories[1–4]. In particular, archeological samples can be used to assess the impacts of the near-field environment and to study how the corrosion layers on the archeological samples may have formed. The use of vitreous archeological samples as analogues for nuclear waste glasses is limited, however, because the precise corrosion environment (e.g., temperature, hydraulic saturation, etc.) is unknown and archeological samples differ in comparison to modern day industrial compositions. Therefore, there remains an opportunity to compare results obtained from short-term laboratory tests to the surface characteristics of archeological samples.

To this end, vitrified samples from the ~1500-year-old Broborg hillfort in Sweden have been extensively studied[1,5,6]. The samples from Broborg are unique and can be compared with archeological[2,7–11] and natural glasses[9,12–14] that have been used as analogues to understand the long-term corrosion behavior of vitreous materials for nuclear waste immobilization. In addition, studies of the corrosion of vitreous materials is also of interest from the perspective of cultural heritage[15,16]. From the collection of studies across the diverse disciplines, there is general consensus that glass corrosion rates in the presence of aqueous solutions are initially high and slow to a residual dissolution rate. This rate drop is related to increasing concentrations of glass constituents in solution, and to the formation of an alteration layer on the glass surface that acts as a passivation barrier. In some instances, the residual rate may continue for the lifetime of the material, or a rate increase may occur due to the formation of certain alteration phases. It is likely that existing archeological samples have corroded at the residual rate for the majority of their lifetime. Further details on the main processes occurring during the alteration of vitreous materials are given in a wide number of reviews on the subject (e.g.,[17,18]).

At Broborg, local granitoid rocks were fused together with melted amphibolite to make the vitrified hillfort walls. In the present study, we synthesized two sets of laboratory samples with equivalent chemical compositions to the archeological samples and subjected them to a set of standard laboratory durability tests. The first set of laboratory samples was synthesized by melting granitic and amphibolitic rocks from Broborg to represent the source materials that the Iron Age people used to make the vitrified archeological samples. The second set of laboratory samples had the same chemical compositions as the granitic and amphibolitic rocks but were synthesized by melting laboratory oxide chemicals. These two sets of laboratory samples were prepared to assess if glasses from melting granitic and amphibolitic rocks gave the same Product Consistency Test (PCT) response as glasses of the same composition synthesized by melting laboratory oxide chemicals. In addition, the tests were used to assess if the presence of crystalline phases, which are present in certain samples, affected the PCT response. This would allow us to use laboratory oxides to make glasses for subsequent durability tests instead of using rocks excavated from the archeological site. The amphibolite and granite rocks were collected from the Broborg site during the 2017 excavation described elsewhere[6,19]. Bulk sample analysis of the granite and amphibolite rocks was presented in Ogenhall[20]. The Broborg site rocks used in this study

---

[1]Energy and Environment Directorate, Pacific Northwest National Laboratory, Richland, WA 99354, USA. [2]US Department of Energy, Office of River Protection, Richland, WA 99352, USA. [3]Smithsonian Institution, Museum Conservation Institute, 4610 Silver Hill Road, Suitland, MD 20746, USA. [4]School of Engineering, Vanderbilt University, Nashville, TN 37235, USA. [5]School of Mechanical and Materials Engineering, Washington State University, Pullman, WA 99164, USA. [6]Department of Materials Science & Engineering, The University of Sheffield, Sheffield S1 3JD, UK. [7]Luleå University of Technology, SE-971 87 Luleå, Sweden. ✉email: james.neeway@pnnl.gov

were melted at several temperatures ranging from 1250 to 1400 °C.

The standard durability tests examined in this study were the PCT[21], the vapor hydration test (VHT)[22], and the United States Environmental Protection Agency (EPA) Method 1313 test[23]. The PCT tests included the standard 7-d PCT-A as well as a modified PCT-B, which allows the test to be carried out at different glass-surface-area-to-volume (S/V) ratios and longer than 7 days. In the present study, we use a modified PCT-B as solution is periodically sampled from the test reactor instead of termination of a test reactor upon sampling. The EPA 1313 test is a room temperature test conducted with a 1:10 mass material:mass solution ratio for 2 days with constant tumbling. The initial solution pH is adjusted so that the final pH of the test falls in a desired target range after reaction with the test material.

To compare the behavior of samples melted in the laboratory with that of vitrified materials from the Broborg site, where the amphibolite and granite were melted together in situ, a previously excavated sample (named BB1b)[24] was also analyzed. The samples melted in the laboratory from rocks or oxides were subjected to PCT, VHT, and EPA 1313, whereas the vitrified material from Broborg was only subjected to VHT. Alteration rates and features were examined through solution analysis and solid phase characterization for samples subjected to PCT, VHT, and EPA 1313. The alteration layer thickness and alteration features from samples excavated from the Broborg site are compared to calculated surficial layer thickness and surficial features from samples altered in laboratory tests.

Information on the vitrification of the amphibolite and granite to form the walls at the Broborg hillfort can be found elsewhere[25]. Briefly, pieces of amphibolite were intentionally placed between the granitoid boulders. As the amphibolite melted during firing, gases released from the melt process were trapped in bubbles and the resulting melt expanded to fill the space between the granitoid boulders, inducing contact melting of the granite and solidifying the vitrified wall upon cooling. The crystalline heterogeneity of the Broborg site samples, discussed in McCloy et al.[26], and the variation in alteration features, presented in Matthews

et al.[27], make interpreting the alteration behavior as a function of natural weathering processes a complex endeavor.

In the present study, three rock samples representative of the source material for vitrification at Broborg were selected to assess the influence of chemical and mineralogical heterogeneity on the alteration behavior of the materials that were produced from them. A previous study with Broborg rocks indicated that the fraction of amorphous content increases when the samples are melted at increasingly higher temperatures[26]. The Broborg glasses contain most of the major elements present in the glasses used for the immobilization of radioactive waste, however the proportions differ (e.g., the Broborg glasses are lower alkali, and higher in silicon (Si), aluminum (Al) and iron (Fe)). In addition, the Broborg samples lack boron (B), which is a significant component of low-activity waste (LAW) glass. However, the Broborg samples are still useful in understanding alteration rates and features of amorphous aluminosilicate materials.

The amphibolite rocks that were chosen were denoted: (i) BA5, from an outcrop ~3 km from Broborg; and (ii) Dike, a dolerite/diabase sample from just beneath the walls at Broborg. The Dike sample melted at a lower temperature than other amphibolite materials obtained from the region surrounding Broborg (see McCloy et al.[26] for more details). The BA5 and Dike samples are primarily composed of amphibole and feldspar, with BA5 having minor amounts of biotite/chlorite and quartz[26]. When melted above 1000 °C, the amorphous fraction in the samples increases and minor (<10 wt%) amounts of magnetite (spinel) are present[26].

Melting the amphibolite samples at 1250 °C produced glasses with similar characteristics to the Broborg sample (BB1b) while remelting at 1400 °C produced a sample with minimal crystalline inclusions. A sample of the local granitoid rock, denoted 443 Granite, was also selected. The granite from the site is mainly composed of feldspar and quartz and, like the amphibolite samples, the amount of glassy fraction increases when the melt temperature increases[26].

There was an oxidizing atmosphere during the melting in the laboratory while at Broborg the atmosphere was likely reducing during vitrification due to heating using charcoal[26]. As ferric iron (Fe^{3+}) is considered a network former and ferrous iron (Fe^{2+}) is considered a network modifier, which promotes non-bridging
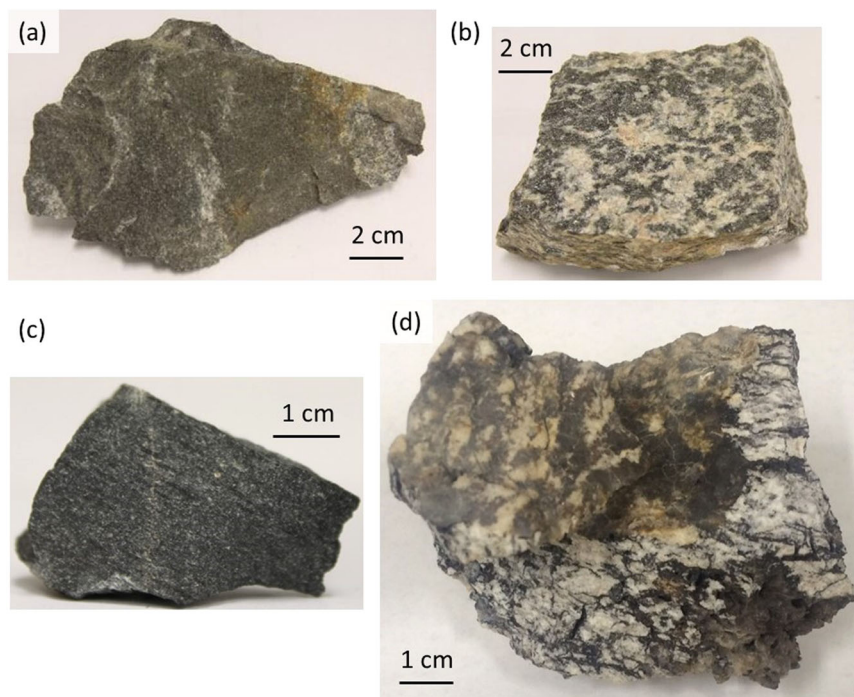

Fig. 1 Photographs of the samples collected from Broborg. a BA5 amphibolite, (**b**) 443 Granite, (**c**) Dike amphibolite, (**d**) BB1b.

oxygen when it adopts an octahedral coordination with oxygen, this may have an influence on the durability of the glass. Photographs of the samples collected from Broborg are provided in Fig. 1, while the measured compositions of the rock samples, through various solid digestion techniques are provided in Table 1. The measured compositions are compared to values from similar site samples that were melted at 1200 °C as part of another study on samples from the Broborg hillfort[26].

RESULTS AND DISCUSSION
Surficial features of Broborg archeological glass
SEM-EDS of a section through BB1b (Fig. 2) shows the heterogeneity of the sample and the surficial features. In BB1b, lighter, high atomic number euhedral crystals of metal oxides are distributed in the glassy matrix. The exposed outer surface of the sample shows evidence of an surficial layer in contact with the environment. This feature is not observed on the internal surface of the void. EDS chemical mapping shows a surface layer enriched in Si compared to the bulk material, and containing Al, Na and K, but in depleted amounts relatively to the bulk, and very little Ca, Fe or Mg. The maximum thickness of the surficial feature is 62 μm, the minimum thickness is 0.5 μm, and the average thickness is 16 μm.

Glass melting experiments
The amphibolite and granite rock samples used for laboratory testing in the present study were excavated at or around the Broborg site (BA5, Dike, and 443 Granite). In addition to the materials produced by melting these rock samples, glasses of the same composition (Table 1) but made from laboratory chemicals, were tested to assess the role of heterogeneity (i.e., crystallinity) on the alteration process. The homogeneity of the glasses was also influenced by melting at different temperatures. The 443 Granite samples melted at 1250 °C produced a sample with remaining quartz and feldspar crystals, while a melt at 1400 °C produced a sample with only minor amounts of quartz and tridymite remaining (Supplementary Figs. 1 and 2). The Dike

sample melted at 1300 °C produced a material that contained only minor amounts of quartz and magnetite (Supplementary Fig. 2).

The melting of the additional samples was done under controlled conditions in the laboratory (refer to the Glass Melting Experiments in the Methods section for more detail). Samples IDs used here include the material and melt temperature (e.g., BA5 1250 °C) while lab-made is used to identify samples produced with lab oxides. A summary of all the samples, along with description of why they are of interest to the present study and the durability tests to which the samples were subjected, is provided in Table 2.

Product consistency test (PCT-A) results
As the archeological samples are rare and have cultural heritage value, conservation of the samples is a priority. One of our aims was to see if laboratory-made samples with identical compositions to those found in the field could be used as a replacement for samples excavated at the site. Six samples [Table 2: BA5 (both 1250 °C and 1400 °C), 443 Granite (both 1250 °C or 1400 °C) and lab-made BA5 and 443 Granite] were subjected to the PCT-A in duplicate for 7 days at 90 °C (PCT was not performed on the Dike 1300 °C sample as the BA5 sample was sufficiently representative of the influence of homogeneity in an amphibolite sample). Though the test is not meant to predict the long-term alteration behavior of glasses, it can be used to assess the relative durability of: (i) glasses of different composition; and (ii) glasses with different levels of heterogeneity, i.e., the presence or absence of crystals.

The concentrations of major ions (Al, Na, K, Si) present in solution after the test were measured by inductively coupled plasma-optical emission spectroscopy (ICP-OES) and are presented in Table 3. Table 3 also includes the normalized elemental mass loss for one square meter of sample surface area (NL$_i$, see Eq. 2 in Methods) and the theoretical alteration thickness (AL$_i$, see Eq. 3 in Methods), which can estimate the surface retreat of the sample indexed to a given element (i.e., the estimated alteration layer thickness).

PCT data were used to assess the relative durability of the different compositions and different levels of homogeneity, i.e., the glasses produced by melting rock samples or laboratory

Table 1. Measured composition determined through a chemical digestion of BA5 amphibolite, Dike amphibolite, and 443 Granite, along with a representative low-activity waste glass (LAWA44)[36].

Oxide	BA5 (amphibolite)	BA5 1200 °C[a]	Dike (amphibolite)	Dike 1300 °C[b]	443 Granite	White Granite 1200 °C [a]	LAWA44
SiO$_2$	46.00	53.46	48.84	53.46	69.42	61.25	44.53
Al$_2$O$_3$	18.45	10.44	13.60	12.77	15.03	21.65	6.20
Na$_2$O	1.75	1.39	2.68	2.78	3.45	6.03	19.99
Fe$_2$O$_3$	13.05	12.19	12.41	12.83	3.41	0.20	6.98
CaO	10.30	12.46	9.10	8.75	2.81	1.25	1.99
K$_2$O	1.67	0.44	1.22	1.39	3.62	6.47	0.5
MgO	4.79	8.45	6.77	6.68	0.85	0.05	1.99
MnO	0.18	0.25	0.30	0.43	0.07	---	0.00
P$_2$O$_5$	0.46	---	0.21	0.20	0.13	---	0.03
TiO$_2$	1.47	0.91	0.87	0.89	0.4	---	1.99
Others[c]	1.74	---	0.48	0.07	---	---	15.84
LOI[d]	1.63		-		0.66		--
Total[e]	99.86	100.00	96.91	100.25	98.85	96.61	100

The relative uncertainty for the major oxides (≥5 wt%) is ±10% and the relative uncertainties for the minor oxides (<5 wt%) is ±20%.
[a]Values from McCloy et al. [26].
[b]Values measured by EPMA.
[c]Others include BaO, B$_2$O$_3$, Cl, Cr$_2$O$_3$, Cs$_2$O, CoO, CuO, F, La$_2$O$_3$, PbO, Li$_2$O, MoO$_3$, NiO, Re$_2$O$_7$, SrO, SO$_3$, SnO$_2$, WO$_3$, V$_2$O$_5$, ZnO and ZrO$_2$
[d]Lost on ignition.
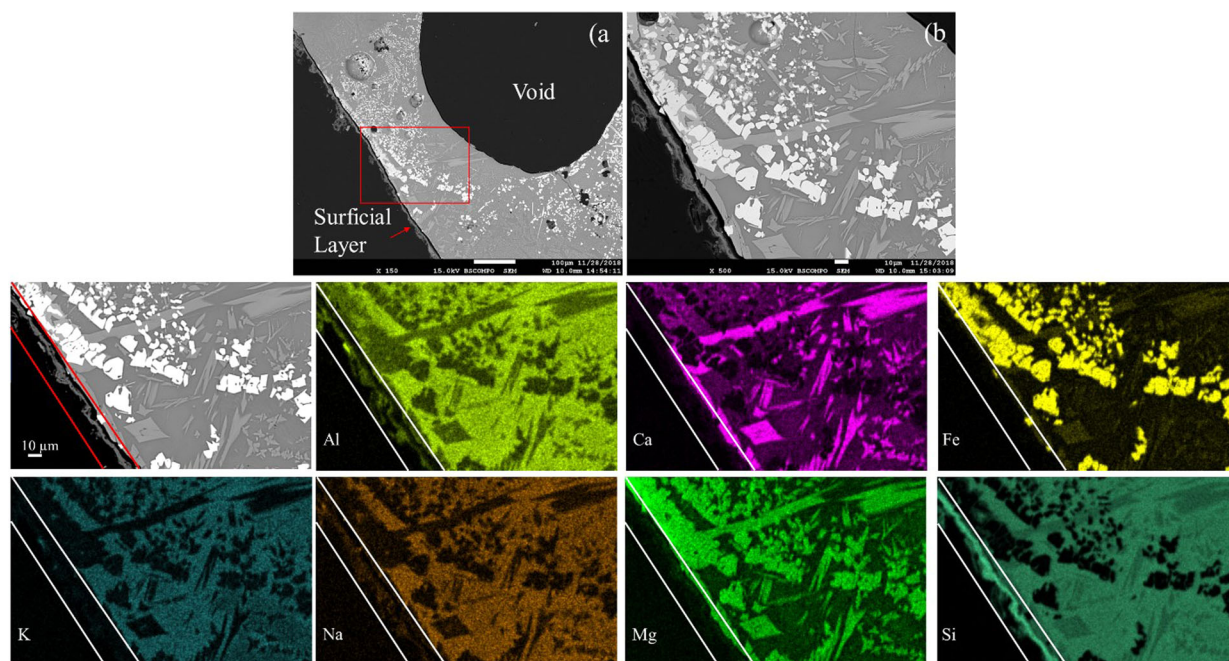[e]Values do not sum to 100.0 due to analytical uncertainties.

Fig. 2 SEM/EDS images showing heterogeneity and surficial features of BB1b. a BB1b showing a surficial layer on the sample along with a void that has not been exposed to the near-field environment (scale bar is 100 μm). **b** A magnification of the area in the red box from (**a**) (scale bar is 10 μm). The EDS maps showing the distribution of major elements in a subsection of (**b**) are shown below with lines to guide the location of the surficial layer (scale bar is 10 μm).

oxides at 1250 °C (inhomogeneous) or 1400 °C (homogeneous). The 7-d PCT results show that the glasses exhibit similar NL_i values irrespective of chemical composition and homogeneity from different melt temperatures. The NL_i values for BA5 for Na and K exceed those for Si and Al indicating that while the more soluble Na and K are released into solution, the less soluble Si and Al likely make up the alteration layer. In the Granite sample, the Na is released in excess of K, Si, and Al. The reason for the relatively low release of K in comparison to Na in the sample is unknown; however, K has been shown to be present in the alteration layer at a greater extent than other alkalis in previous studies[28].

The rate of alteration is calculated and compared with those for the other tests in the Discussion section. In general, the calculated alteration depth was <0.1 μm for the six glasses. This is near the limit of the spatial resolution achievable with SEM. The results of the normalized mass loss for all six samples are well below the maximum established US PCT-A limits for high-level waste glass ($NL_B = 8.35\ g\ m^{-2}$, $NL_{Na} = 6.67\ g\ m^{-2}$, and $NL_{Li} = 4.78\ g\ m^{-2}$)[29,30] and LAW glass (NLB, NL_{Na}, and $NLSi < 2\ g\ m^{-2}$)[31].

Collectively, the results demonstrate that the Broborg materials are much more durable than nuclear waste glasses, supporting the observation that the vitrified part of the hillfort wall at Broborg has remained relatively unaltered for ~1500 years.

Modified product consistency test (PCT-B) results

The 7-d PCT-A tests provided a general assessment of the durability of the various materials. However, because the alteration layers were extremely small and the test duration was short, the test did not produce observable alteration layers using standard characterization techniques, such as SEM. Thus, additional tests were conducted at a lower S/V (200 m^{-1}) and longer times (up to 90 days) with periodic sampling to generate thicker alteration layers. Figure 3 provides the NL_{Si}, NL_{Na}, and NL_{Al} values from the modified PCT-B of the same samples that underwent PCT-A. Complete solution and test data are provided in Supplementary Table 1. At the end of the 90-d test, the NL_i for Na, Si, and Al for granite samples were within agreement with one

another and NL_i for Na, Si, and Al for BA5 were also within agreement with one another. However, there are some trends in the data:

1. The laboratory-made granite glass NL_{Si} value is about 1.5× greater than the melted 443 Granite throughout the test duration. This may be due to the slightly higher pH of the laboratory-made sample solution (8.1 ± 0.1) compared to solutions containing the material from melted rock (7.8 ± 0.1 for both the 1250 °C and 1400 °C) or due to the slight differences in the glass structure and homogeneity resulting from using rocks vs. laboratory chemicals.

2. The time for the samples to approach a quasi-equilibrium with solution is longer for the 443 Granite compared to BA5. This is especially evident for NL_{Si} and NL_{Al} values for BA5 where the Si value does not appear to change after 3 days. On the other hand, the NL_{Si} and NL_{Al} values for 443 granite show a gradual increase until around 40 days when a relatively steady state is achieved. These trends mostly agree for the NL_{Na} with the exception that the NL_{Na} values for BA5 continue to increase for the duration of the experiment even as the pH stabilized at pH_{RT} near 8.4 (see Tables S2 and S3).

3. The NL_{Si} values for the 443 Granite and BA5 samples are nearly equal at the end of the experiment even as the SiO_2 concentration in the granite sample is 1.5× greater than the BA5 sample. This suggests that there is consistent solubility control of Si in the two types of silicate materials. The average Si concentration from all durations for all samples was 15 ± 4 ppm, which is near the solubility of quartz at pH 8 and 90 °C (20 ppm Si). However, as quartz is unlikely to precipitate under these conditions, this is likely a coincidence and the phase controlling Si concentrations merits further investigation.

4. The NL_{Al} values for BA5 are both lower than the 443 Granite and decrease slightly with time. The trend for NL_{Al} for granite is similar to NL_{Si} and NL_{Na}, in that the release is initially fast and then slows with time, but the BA5 NL_{Al}

Table 2. Melt history of each of the seven samples prepared for chemical durability testing.

Sample ID	Melt temperature (°C)	Melt time	Melt notes	General notes	Tests
BA5 1250 °C	1250	1 h		Purpose was to reproduce melt conditions and heterogeneity (presence of crystals) found in Broborg samples. Many inclusions of unmelted quartz.	PCT, VHT, EPA 1313
BA5 1400 °C	1400	Two melts at 1 h each	Crushed to fine powder between melts	Some inclusions of quartz in the vitreous portion.	PCT, VHT
Lab-made BA5	1400 (1st melt) 1450 (2nd melt)	Each melt at 1 h each	Crushed to fine powder between melts	Homogeneous sample.	PCT, VHT
443 Granite 1250 °C	1250	1 h		Purpose was to reproduce melt conditions and heterogeneity (presence of crystals) found in Broborg samples; glass only found in localized area; large quartz grains remain.	PCT, VHT
443 Granite 1400 °C	1400	Two melts at 1 h each	Crushed to fine powder between melts	Many inclusions of quartz throughout vitreous fraction.	PCT, VHT
Lab-made Granite	1400 (1st melt) 1450 (2nd melt)	Each melt at 1 h each	Crushed to fine powder between melts	Opacity caused by numerous micron-sized bubbles. Bubbles too small to remove from viscous melt.	PCT, VHT
Dike	1300	1.3 h	No unmelted particles observed by optical microscopy	Some crystalline material on a micrometer scale (Fig. S1).	VHT

The samples listed here were melts from rock samples excavated directly from the site or made in the lab from lab chemicals (i.e., lab-made'). The Tests column provides the durability tests to which the samples were subjected.

values slightly decrease. This may be due to Al precipitating at the glass surface; however, we did not observe an Al-rich layer from the SEM-EDS analysis. The average Al concentration from all durations for all samples was 5 ± 1 ppm, which higher than the solubility of gibbsite at pH 8 and 90 °C (0.5 ppm Al).

Vapor hydration test (VHT) results

Six coupons [Table 2: BA5 (both 1250 °C and 1400 °C), 443 Granite (both 1250 °C or 1400 °C) and lab-made BA5 and 443 Granite] were subjected to the VHT in duplicate at 200 °C for 24 days. VHT was also performed on the vitrified archeological Broborg glass sample, BB1b, cut to the desired coupon dimensions, so that the chemistry and morphology of the surficial phases could be compared with those in Fig. 2. Prior to testing, the BB1b sample was prepared by removing the altered surface where possible. Images of VHT coupons before reaction are provided in Supplementary Fig. 3. The VHT is performed to accelerate the alteration process and identify solid alteration phases on a surface over a short period of time[32]. Previously, the phases identified from the high-temperature VHT with a Hawaiian basaltic glass were demonstrated to be similar to alteration products from naturally altered samples (primarily an amorphous layer enriched in Fe and Ti and some clays)[33,34]. Vapor hydration tests (VHTs) have also been used to understand practices related to conservation of glasses related to cultural heritage[9].

After the VHT, optical microscopy revealed a cloudiness on all the glass surfaces indicative of alteration (Fig. 4a and c). Cross-sections of the 24-day VHT samples were examined by SEM to assess the thickness and morphology of the alteration layers. On some samples, the alteration layers were too small to be examined by SEM. The heterogenous (i.e., crystal-containing) material obtained by melting BA5 amphibolite to 1250 °C had an alteration layer 2–4 µm thick with alternating layers of increased porosity (decreased density) as shown by the alternating dark and light layers in the alteration layer on the glass surface (Fig. 4b); however, the alternating layers may be related to exfoliation of the alteration layer upon specimen preparation in the epoxy. The homogeneous sample obtained by melting 443 Granite to 1400 °C showed a porous region at the interface between the unaltered material and the alteration layer and had an alteration layer thickness between 1 and 30 µm (Fig. 4d; portion in image shows a layer 6–8 µm thick). This small amount of alteration contrasts with LAW glasses that typically have an alteration thickness on the order of mm for the 24-day test at 200 °C[32].

Based on these results, 49-day VHTs were conducted at 200 °C with samples produced by melting the BA5 at 1250 °C and the Dike at 1300 °C. The VHT was performed for twice as long with the aim of generating an alteration layer more than twice as thick, because an induction period where the reaction rate is initially slow can occur, then reaction rate increases rapidly after certain alteration phases form[34,35].

The BA5 1250 °C coupon after the 49-d VHT is shown in Fig. 5. Examination by optical microscopy (Fig. 5b) shows bubbles, cracks and unmelted quartz on the coupon surface that were also present on the pre-reaction coupon (Fig. 5a, inset). Cross-sectional SEM analysis showed an alteration layer with an average thickness of 11 µm that is continuous and follows the contours of bubbles present at the surface (Fig. 5c). This corroded layer continues in cracks that extend >10 µm into the sample (Fig. 5d).

The Dike coupon after the 49-d VHT is shown in Fig. 6a. The test resulted in a distinct color change compared to the pre-reaction coupon in the inset, indicated by the formation of yellow precipitates on the surface, but no evidence of crack formation. SEM analysis shows a surficial layer, 4–40 µm thick, that extends from the original surface to the edge of the sample surface.

Table 3. Concentrations, NL_i values, and alteration depth results from 7-day PCT (average of duplicate samples) for different materials used in this study (Dike excluded).

Material	Preparation	Value	Al	Na	K	Si
BA5 (Amphibolite)		conc., mg L^{-1}	3.0 ± 0.3	3.0 ± 0.3	2.7 ± 0.3	16 ± 2
	1250 °C	NL_i, (×10^3 g m^{-2})	16 ± 2	120 ± 10	97 ± 12	37 ± 4
		AL_i, nm	6.0 ± 0.8	43 ± 6	36 ± 5	14 ± 2
		conc., mg L^{-1}	3.1 ± 0.3	2.3 ± 0.2	2.0 ± 0.2	13 ± 1
	1400 °C	NL_i, (×10^3 g m^{-2})	16 ± 2	89 ± 12	73 ± 10	30 ± 3
		AL_i, nm	6.0 ± 0.8	33 ± 5	27 ± 4	11 ± 1
		conc., mg L^{-1}	2.9 ± 0.3	2.5 ± 0.3	2.2 ± 0.2	14 ± 1
	Lab. Oxides	NL_i, (×10^3 g m^{-2})	15 ± 2	96 ± 13	80 ± 11	33 ± 3
		AL_i, nm	6.0 ± 0.7	36 ± 5	30 ± 4	12 ± 1
443 Granite	1250 °C	conc., mg L^{-1}	5.9 ± 0.6	7.4 ± 0.7	0.91 ± 0.09	21 ± 2
		NL_i, (×10^3 g m^{-2})	37 ± 4	110 ± 10	6.2 ± 1.5	33 ± 3
		AL_i, nm	14 ± 2	39 ± 5	2.0 ± 0.6	12 ± 1
	1400 °C	conc., mg L^{-1}	5.0 ± 0.5	5.3 ± 0.5	0.85 ± 0.1	24 ± 2
		NL_i, (×10^3 g m^{-2})	31 ± 3	76 ± 8	5.8 ± 1.5	39 ± 4
		AL_i, nm	11 ± 1	28 ± 3	2.0 ± 0.6	14 ± 2
		conc., mg L^{-1}	9.3 ± 0.9	17 ± 2	4.6 ± 0.5	38 ± 4
	Lab. Oxides	NL_i, (×10^3 g m^{-2})	58 ± 6	240 ± 20	31 ± 3	60 ± 6
		AL_i, nm	21 ± 2	89 ± 10	12 ± 1	22 ± 2

The relative uncertainties for the concentrations are 10%. Relative uncertainties were calculated with Eqs. 4 and 5 for NL_i and depth, respectively.

The amphibolite rock samples, BA5 1250 °C (Fig. 5) and the Dike (Fig. 6), have similar chemistry (Table 1), but exhibit differences in terms of homogeneity after melting. The BA5 1250 °C coupon exhibits μm-scale crystalline heterogeneity, with brighter areas corresponding to μm-sized iron-containing crystals (Fig. 5c and d) and near mm-sized quartz particles as white inclusions (Fig. 5a, inset). The Dike coupon is homogeneous on the μm-scale (Fig. 6c and d) but exhibits sub-μm-scale crystalline heterogeneity (Supplementary Fig. 4). The differences result in contrasting alteration layer thickness and morphology after exposure to VHT. After a 49-day VHT, the BA5 1250 °C coupon still contains cracks and bubbles (Fig. 5b), but with a precipitated phase that is of similar contrast in the BSE-SEM (i.e., chemistry) to the pristine material (Fig. 5c). However, the surface of the Dike glass coupon after VHT has distinct yellow precipitates, with an alteration layer (4–40 μm) directly beneath that it is darker in contrast (i.e., depleted in elements with higher atomic mass) than the pristine material and the precipitate. Layers of alteration up to 40 μm thick are also shown on the left side of the coupon in Fig. 6c.

Lastly, a 49-day VHT was performed on the archeological Broborg glass sample, BB1b, after the original surficial layer (shown in Fig. 2) had been removed by polishing. SEM analysis of the polished surface (long flat region in Fig. 7c) shows precipitates that likely formed due to reaction of the coupon with water vapor (see surface of Fig. 7d). EDS chemical mapping shows a surface layer enriched in Si compared to the bulk material, as with the alteration layer on the sample altered in the environment (Fig. 2), and containing Al, Na and K, but in depleted amounts relatively to the bulk. A thin Ca film is also seen on the samples. This thin Ca film, along with a heterogeneous distribution of the elements within a thin melt film, was also observed on similar samples characterized by Matthews et al.[27] Unlike the sample altered in the environment, the alteration layers produced by VHT also contained Fe and Mg (Fig. 7).

The morphology of the surficial layers produced on the BBlb glass by VHT did resemble the surficial signatures on the BB1b sample altered in the environment (Fig. 8), despite the conditions of the VHT that are not representative of the natural altering environment. Both samples exhibit a layer that is lighter in contrast (i.e., enriched in higher atomic number elements) at the interface between the glass and the surficial layer (Fig. 8a and b).

However, there were key differences including the depth of the surficial features and the extent of contact between the surficial layer and the surface.

EPA 1313 results

The 2-day, room-temperature EPA 1313 test was performed with BA5 1250 °C and the reference LAWA44 composition[36] to observe similarities and differences in behavior between a melted Broborg sample and a representative LAW glass. The normalized release (NC_i; Eq. 1) of Al, Ca, Fe, Mg, Na, and Si from BA5 1250 °C and LAWA44 from EPA Method 1313 testing are provided in Fig. 9. The natural pH (i.e., resulting pH from the test conducted in deionized water) of the glasses was 8.9 and 9.8 for BA5 and LAWA44 glass, respectively. The concentrations for test condition for each material are provided in the Tables S2 and S3.

The NC_i values from the leaching of Na and Si showed similar shapes—the highest release in acidic conditions, lower release in near-neutral conditions, and a higher release in alkaline conditions. This general response to pH has also been observed with the initial dissolution rate of nuclear waste glasses[37,38]. The NC_i values for Na were systematically half an order of magnitude greater than the NC_i values for Si. The changes in NC_i values for Al is greatest between pH 2 and 6, where the release decreases by four orders of magnitude, and between pH 6 and 13, where the NC_i values for Al increase by three orders of magnitude. The minimum NC_i value for Al is slightly lower for LAWA44 than for BA5 1250 °C, but the equivalent pH 6 data point for LAWA44 was not collected for BA5 1250 °C. NC_i value for Ca, Fe, and Mg were highest in acidic conditions and decreased with increasing pH. Iron is the element with the most divergent release behavior for BA5 1250 °C and LAWA44 of any of the analyzed elements. This is likely due to the inclusion of highly insoluble crystalline spinel in BA5 1250 °C.

DISCUSSION

The study of vitreous archeological samples altered in the natural environment, including vitrified archeological samples produced by pre-Vikings at the Broborg hillfort ~1500 years ago, is an important part of the overall strategy for predicting the behavior
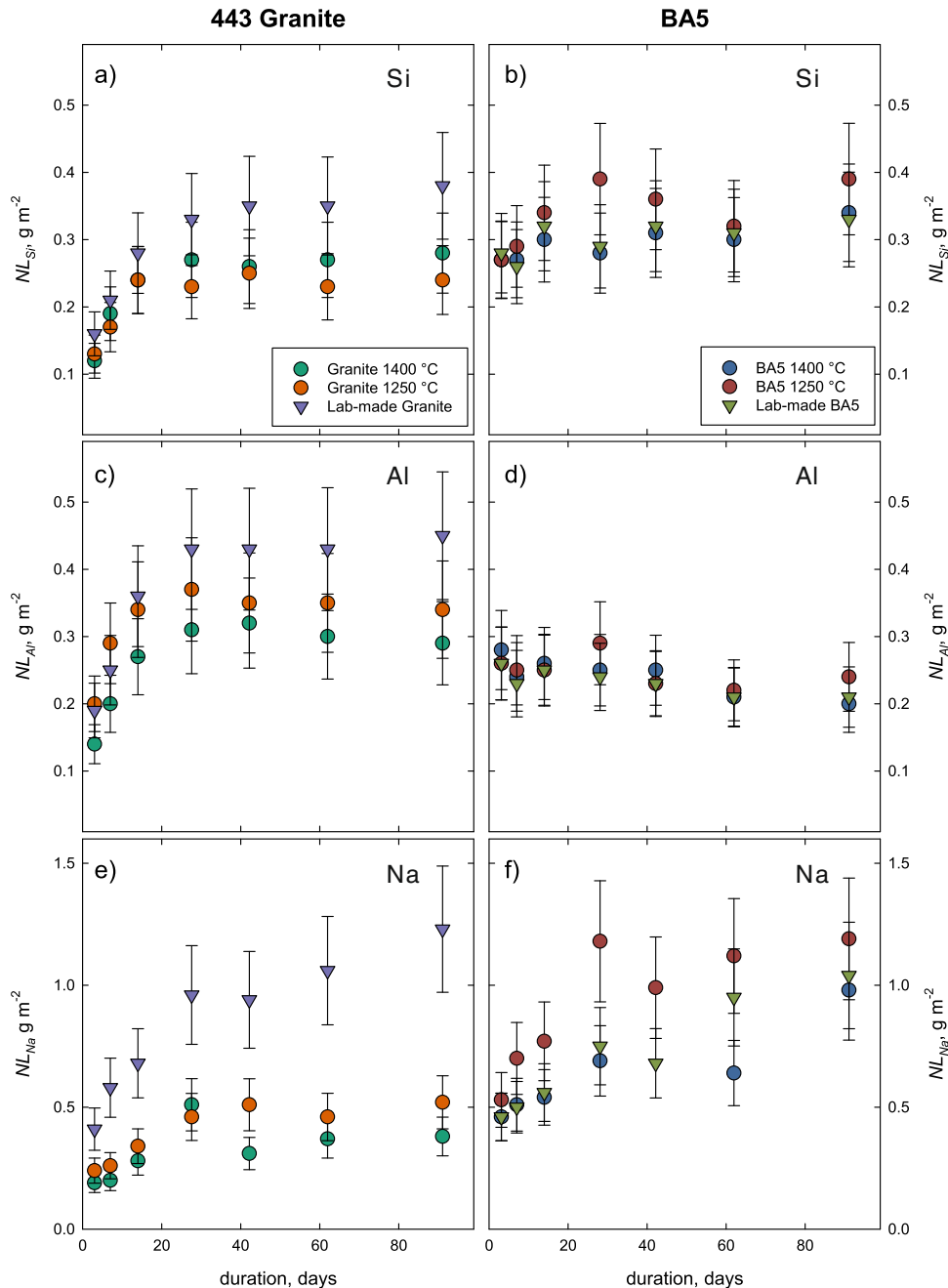
Fig. 3 The normalized mass loss (NL$_i$) for 443 Granite and BA5 samples from modified PCT-B conducted at 90 °C and 200 m^{-1}. NL$_{Si}$, NL$_{Al}$, and NL$_{Na}$ are plotted in (**a,c,e**) and (**b,d,f**) for Granite 443 and BA5, respectively. The *y*-axis for the Na data (**e,f**) is plotted on a different scale than Si (**a,b**) and Al (**c,d**). The uncertainty displayed in the plots is 21% of the value of NL$_i$ was calculated with Eq. 6.

of materials far beyond the range of laboratory experiments. The concept of glass alteration analogues has been discussed elsewhere[1,39–41]. Here, a series of melting experiments, based on the work described in McCloy et al.[26], was conducted to generate glasses that were representative of Broborg archeological materials, to determine effects of chemical composition and the presence of crystalline phases on alteration behavior. Both melted Broborg samples and lab-made samples were subjected to standard test methods: PCT, VHT, and EPA 1313. The influence of heterogeneity (i.e., inclusion of crystals in the vitreous matrix) was qualitatively examined through the PCT-A and modified PCT-B methods. The response of the Broborg material to the EPA 1313 test was compared with the response of a reference LAW glass. The extrapolation of long-term alteration rates measured with

laboratory tests was compared with alteration rates for vitrified Broborg material altered over hundreds of years in a near surface environment.

Results from the 7-day PCT-A suggest that homogeneous BA5 samples (materials melted at 1400 °C) were within a factor of two compared to BA5 samples that still contained crystalline phases (materials melted at 1250 °C) based on NL$_{Na}$ values. This observation contrasts with previous results where the presence of crystals, notably Si-containing crystals, decreased the durability of nuclear waste glasses[42]. Heterogeneity in a sample may lead to the presence of two phases with different degrees of durability. Materials produced from melting 443 Granite altered less than glass produced from melting laboratory oxides with the same composition. The 7-day PCT-A did not produce alteration layers of
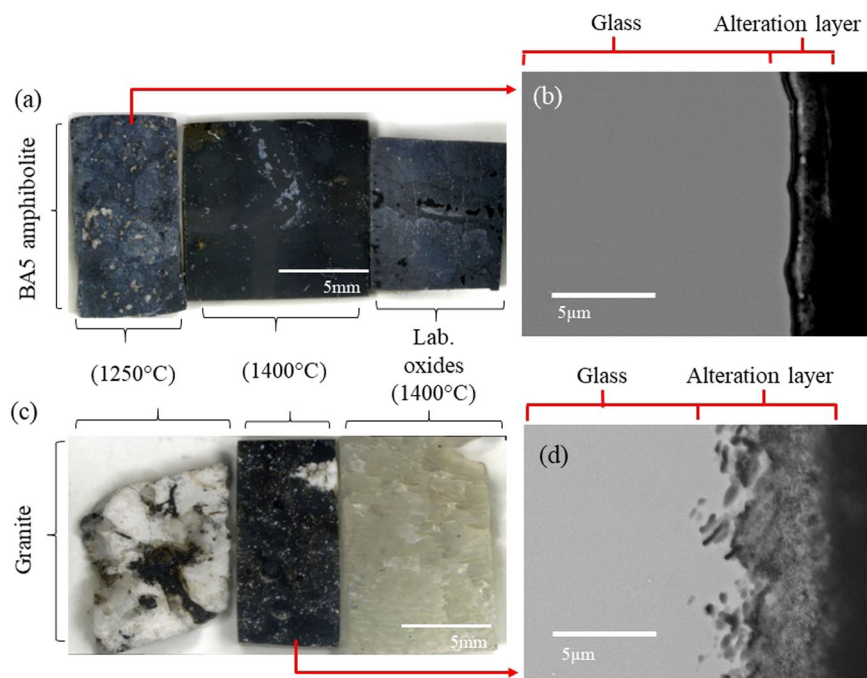
Fig. 4 Post-VHT images of various samples. a Coupons of BA5 amphibolite melted at 1250 °C and 1400 °C, and of laboratory oxides of similar compositions after VHT for 24 days at 200 °C and (**b**) corresponding BSE-SEM of a cross section of BA5 1250 °C. **c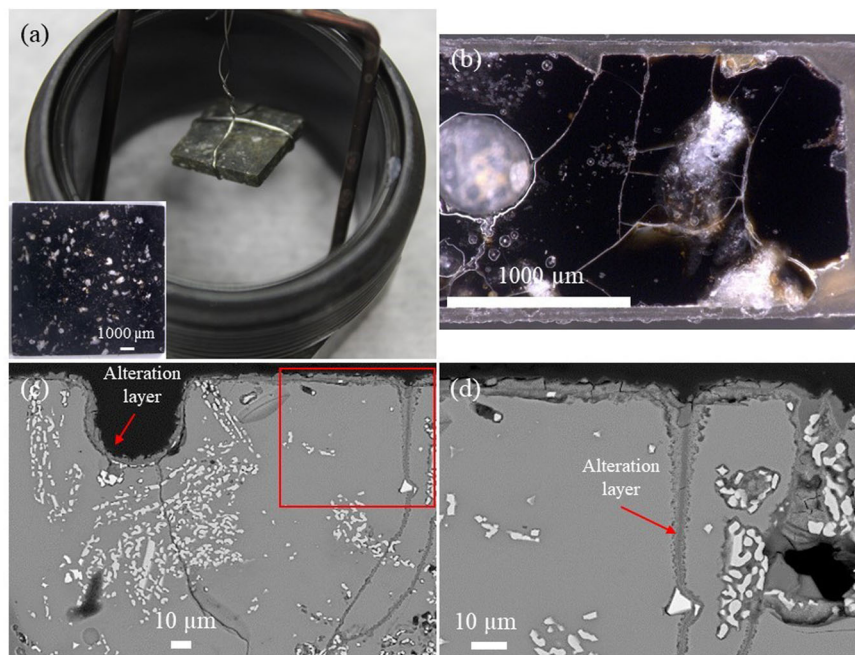** Coupons of 443 Granite melted at 1250 °C and 1400 °C, and of laboratory oxides of similar compositions after VHT, for 24 days at 200 °C (**d**) and corresponding SEM of a cross section of 443 Granite 1400 °C.

Fig. 5 BA5 1250 °C glass coupon after the 49-day VHT. a The post-reaction coupon suspended from the stainless-steel apparatus at the end of the reaction (inset shows pre-reaction coupon), (**b**) optical micrograph of a polished cross section, (**c**) and (**d**) BSE-SEM cross sections at different magnifications (the red box is the area associated with (**d**)).

measurable thickness (by SEM). However, the PCT-A data demonstrated that the materials exhibit NL_i values within a factor of two of one another and one to two orders of magnitude below the LAW NL_i limit irrespective of chemical composition and homogeneity from different melt temperatures or starting materials (laboratory oxides vs. granitic/amphibolitic rocks).

The different chemistry of the granite and amphibolite compositions, and the pH of the solution, appeared to have the greatest effect on PCT-A response.

Tests conducted for 90 days with the modified PCT-B at an S/V ratio of 200 m^{-1} demonstrated that the glass dissolution rate continues to slow until a quasi-equilibrium is achieved after
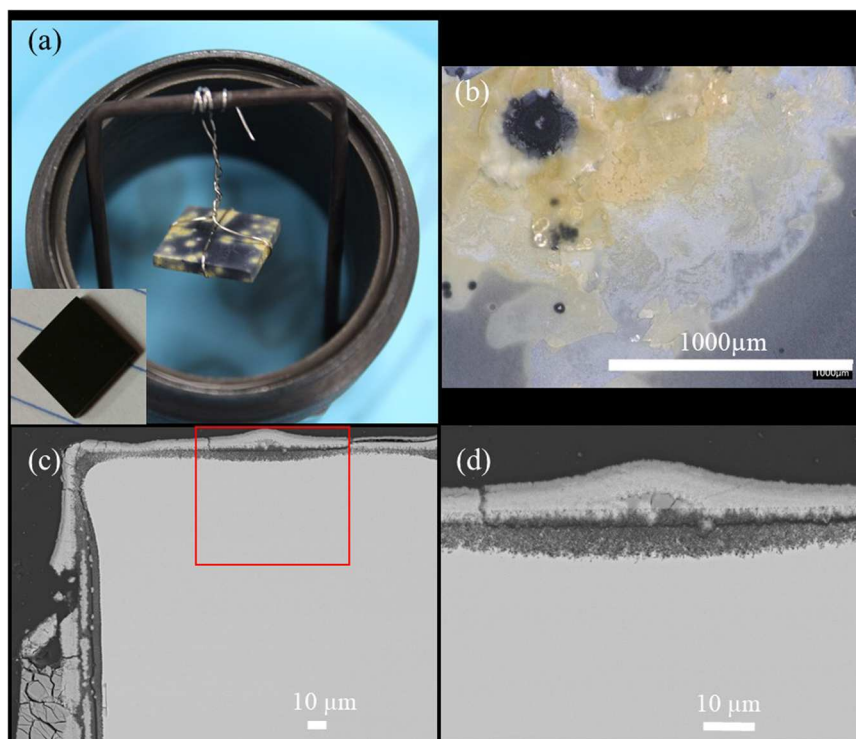
Fig. 6 Dike amphibolite coupon after the 49-day VHT. a The post-reaction coupon suspended from the stainless-steel apparatus at the end of the reaction (inset shows pre-reaction coupon), (**b**) optical micrograph of a corroded area on a coupon surface, (**c**) and (**d**) BSE-SEM cross sections at different magnifications (the red box is the area associated with (**d**)).

almost one month of reaction. The longer-term tests also highlight that the lab-made granite samples were slightly less durable than the materials produced from melted granite. This difference may be related to the homogeneity of the samples. No such difference in durability was observed for the lab-made and BA5 amphibolite samples.

The EPA 1313 test better represents the temperature of near surface disposal conditions and captures the influence of changes in pH, unlike PCT and VHT. When comparing the EPA Method 1313 alteration rate ($\mu m \, yr^{-1}$) to rates from VHT and PCT (Table 4), it should be noted that EPA Method 1313 is an agitated test, while the others are quiescent. Agitation during testing can prevent the buildup of a constituent diffusion boundary layer at the solid-solution interface, which can occur during quiescent testing and slow the observed rate of elemental release. In addition, agitation has the potential to expose fresh surfaces for leaching during particle-particle collisions that would also increase the rate of release.

Similarities from the EPA 1313 test were observed in the pH-dependent leaching behavior of BA5 1250 °C and LAWA44. Specifically, normalized Na, Si, and Mg releases from the two materials were identical within test uncertainty and the release was higher in the low pH and high pH range and lowest in the near-neutral range. On the other hand, at high pH there was some deviation in the release of Mg, Fe, and Ca. All testing results are provided in Table S2 and S3. In addition, the natural pH (i.e., pH resulting from the test conducted in deionized water) of BA5 was 8.9 and LAWA44 was 9.8 likely due to the higher alkali content of LAWA44. As the number of glasses that have been tested by this method thus far is rather small, further testing is required to understand how these results are related to material composition. Specifically, testing a wider range of compositions may allow the effects of various elements to be determined, both in terms of their structural role and their influence in solution. Similar studies have been used to develop models for predicting PCT and VHT

responses as a function of glass composition, and could be conducted for the EPA 1313 test[43]. Additional testing is underway to understand what these results mean in terms of the release of key contaminants into the environment, with the goal to provide a direct link to performance assessment of near-surface disposal of vitrified low-activity radioactive waste.

The limited release of Mg and Ca into solution at high pH is likely due to the formation of highly insoluble hydroxide phases or, in the case of Ca, incorporation into a gel layer to charge balance under-coordinated silicon ($[Si(OH)]^{3-}$ and $[Si(OH)_2]^{2-}$), aluminum $[AlO_4]^-$ and zirconium $[ZrO_6]^{2-}$ in LAWA44[44,45]. Furthermore, secondary (alumino)silicate minerals (e.g., phyllosilicates) containing Mg form readily at pH values above 8[46]. However, slow precipitation kinetics and the low temperature of the test may also inhibit the formation of these phases. At the pH resulting from glass dissolution in deionized water (i.e., natural pH), the normalized release (See Table S3) for Na is 49.9 mg L^{-1} (BA5) and 77.2 mg L^{-1} (LAWA44) and for Si is 19.1 mg L^{-1} (BA5) and 20.2 mg L^{-1} (LAWA44), with a ratio between Na/Si normalized release of ~2.5 to ~4. The higher release of sodium than network forming elements such as Si from both BA5 and LAWA44 suggests an ion exchange process. The normalized release behavior for Fe is distinctly different between the two materials at pH greater than 6, suggesting different leaching and retention mechanisms. This observation of incongruent dissolution at basic pH may be the result of recalcitrant Fe-bearing spinels present in BA5 1250 °C, where the spinel phase is less soluble than the glassy phase[47]. In summary, various mechanisms control release of the alkaline earths and transition metals in neutral to alkaline pH. Deviation from congruent release suggests a solution feedback mechanism, meaning that EPA Method 1313 may not provide a maximum value of a glass dissolution rate.

The calculated thickness of the surficial layers obtained from PCT (Eq. 3) and measured thicknesses from SEM for VHT experiments on materials produced in the lab, and of surficial
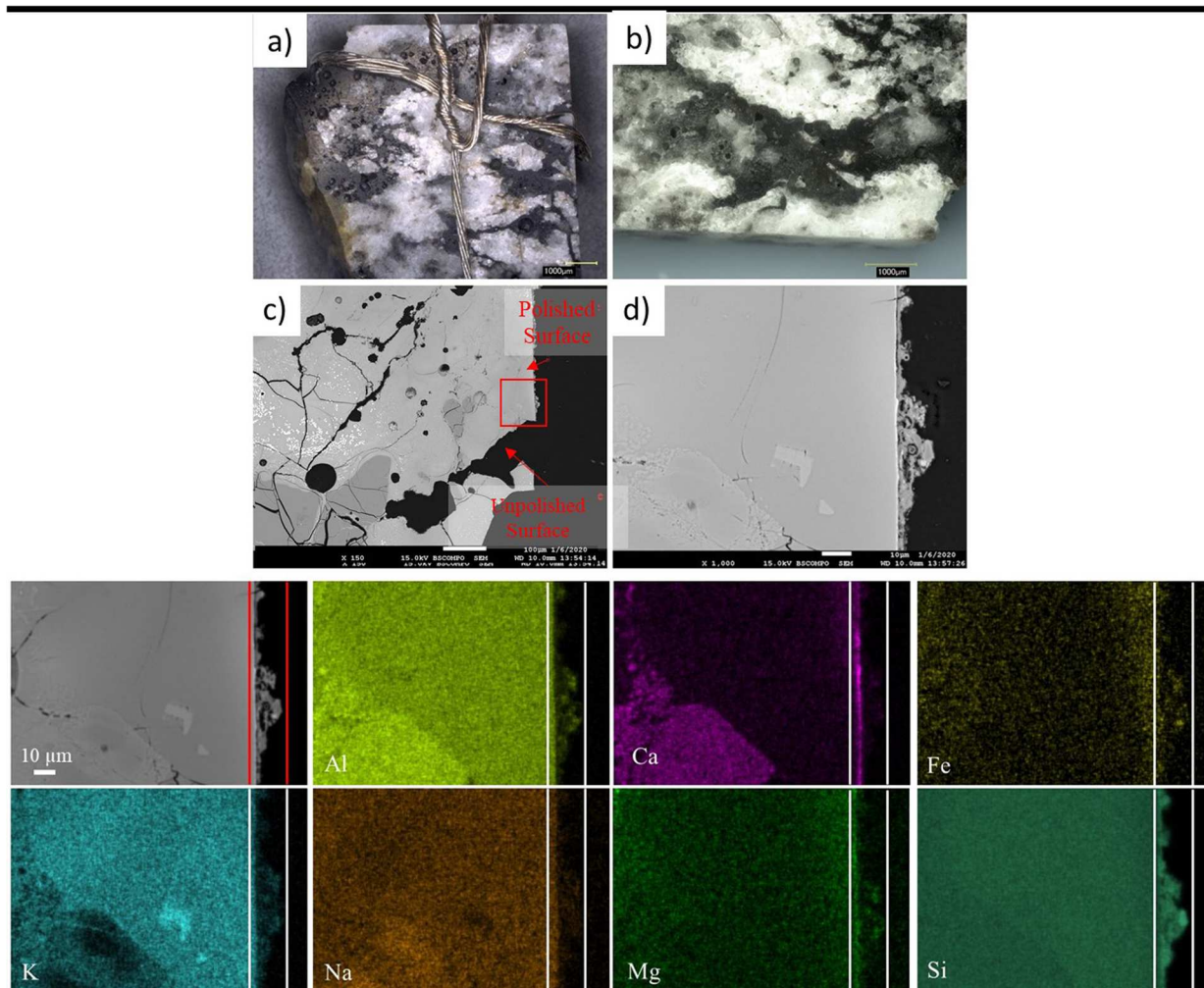
Fig. 7 Archeological sample BB1b after 49-day VHT. a Photograph of pre-reaction coupon with stainless steel wire for suspension in VHT apparatus (scale bar is 1000 µm), (**b**) photograph of sample surface after reaction (scale bar is 100 µm), (**c**) SEM image of a cross section through BB1b (scale bar is 100 µm), (**d**) higher magnification SEM image of area in red box in (**c**). EDS maps (shown below) showing distribution of major elements present at the surface in (**d**).
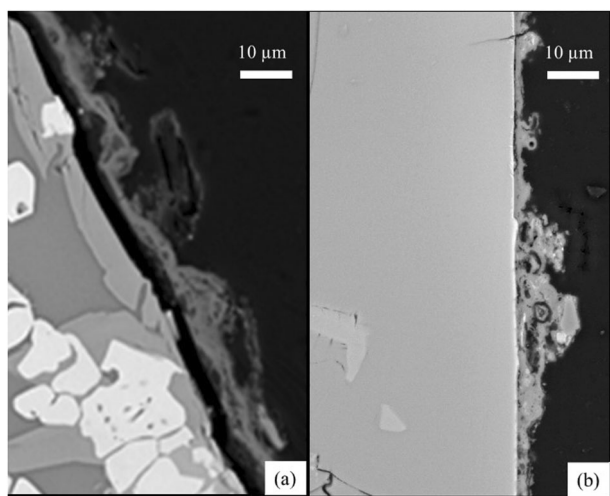

Fig. 8 A comparison of alteration features produced by exposure to the altering environment at Broborg. a Archeological glass samples BBlb (**b**) with alteration features produced by VHT for archeological glass sample BBlb.

layers on a vitrified sample excavated from the site are provided in Table 4. As expected, the PCT produced the thinnest alteration layers. The site-excavated samples had surficial layers of similar morphology to VHT samples despite alteration occurring at vastly different time scales (49-day VHT vs. 1500 years) and temperature (200 °C VHT vs. 5.4 °C). However, the rate of alteration layer formation, which is calculated simply by dividing the surficial layer thickness by test duration, correlates with test temperature. Figure 10 provides an Arrhenius plot of the natural log of the alteration rate of the various samples as a function of the inverse temperature. The activation energy calculated from the slope is 47 ± 5 kJ mol^{-1} generated by the data in Table 4, which is on the low end of values that exist for nuclear waste glass where the rate-controlling mechanism is assumed to be the rupture of the Si-O bond[48]. However, as the glasses from the lab tests and the site samples are likely in different rate regimes, the linear relationship may not apply to the site samples.

The rates measured by EPA 1313 are slightly greater than those predicted by the activation energy by a factor of roughly two. This is likely due to the solution agitation in the EPA 1313 test methods. However, it is unclear if the rates and activation energy determined from PCT and VHT from Broborg samples are orders of magnitude lower than for LAW glasses. The lower rates for the
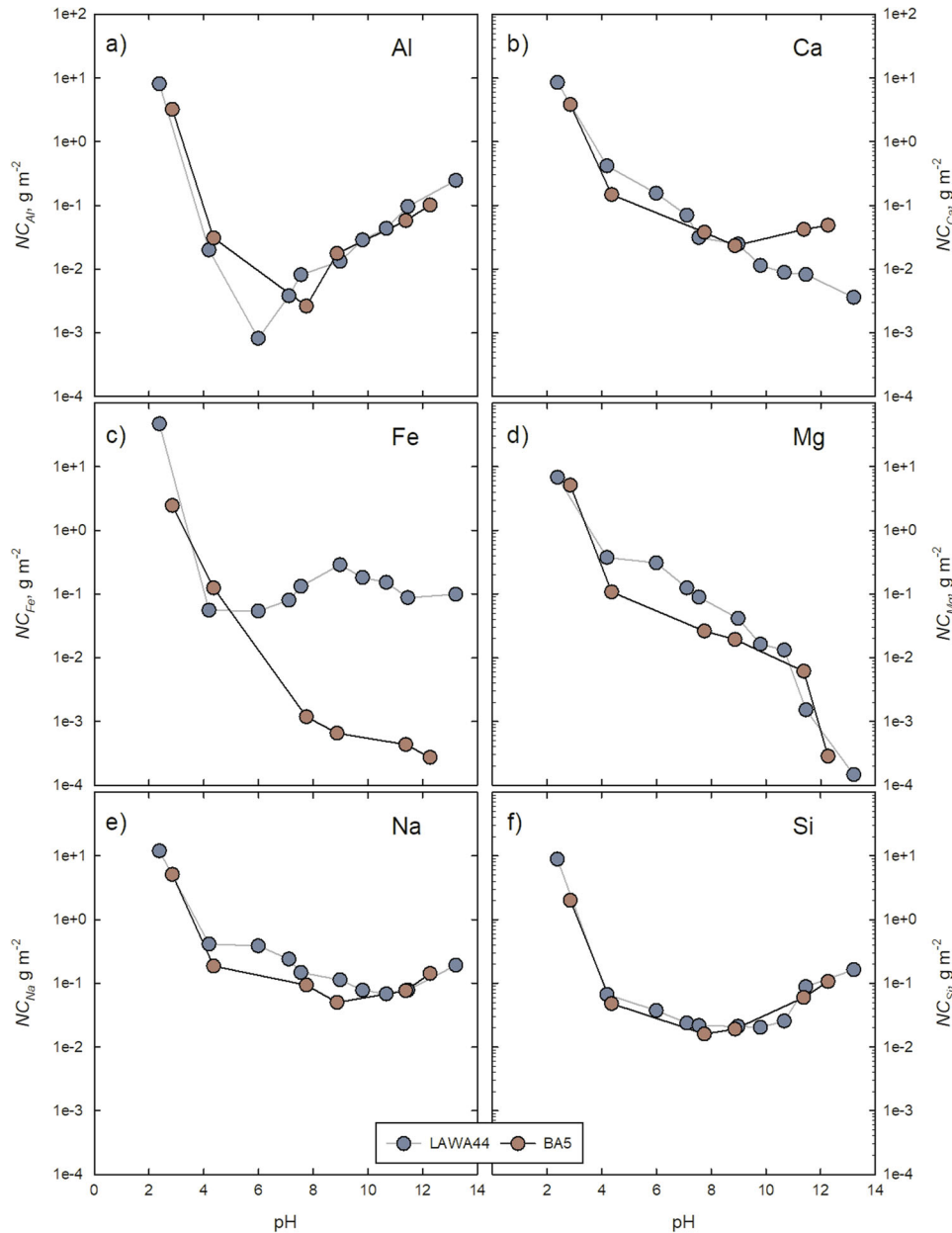
Fig. 9 Normalized release (NC$_i$ in g L^{-1}) for selected constituents as a function of final extract pH from EPA Method 1313 testing of BA5 and LAWA44. a NC$_{Al}$, (**b**) NC$_{Ca}$, (**c**) NC$_{Fe}$, (**d**) NC$_{Mg}$, (**e**) NC$_{Na}$, and (**f**) NC$_{Si}$. The uncertainty (not shown) displayed in the plots is 14% of the value of NC$_i$ was calculated with Eq. 5.

Broborg samples from PCT and VHT data is likely related to the amount of Na and B in the LAW samples. Further investigations are underway to better understand how the addition of these elements would link the behavior of Broborg and LAW samples.

A comparison of the alteration layer produced on the BBlb by VHT with the surficial features produced by exposure to the environment at Broborg for BBlb (Fig. 8), reveal similarities in terms of the texture, despite the harsh temperature conditions of VHT. Both samples exhibit a layer that is lighter in contrast (i.e., enriched in higher atomic number elements) at the interface between the glass and the surficial layer (Fig. 8a and b), though it is much thinner for the VHT sample than for the sample altered in the environment. There are other differences; for example, the surficial layer produced by VHT directly contacts the glass in most cases (Fig. 8b), but there is a gap between the surficial layer and the glass on the naturally altered BBlb (Fig. 8a). These differences

may be due to the lack of liquid water in the VHT, which could carry away soluble elements in the altering environment at Broborg, or to differences in how well the surficial layer adheres to the glass. Here, examination of the chemistry and morphology of the surficial layers revealed that they are thin and heterogeneous. This suggests that the glasses are highly durable, and that the mechanisms responsible for the formation of these heterogeneous features are complex and variable. Work is ongoing to determine how the chemistry of the samples, and of the altering environment, combine to influence the long-term alteration behavior of these samples.

In conclusion, this work has shown that standardized chemical durability laboratory tests conducted at high temperature can reproduce surficial features that are similar in morphology to those produced under environmental conditions. It has also been demonstrated that an Arrhenius relationship links reaction rates

Table 4. Summary of aging types, durations, temperatures, surficial layer thicknesses, and alteration rates for samples discussed here.

| Glass sample | Aging type | Duration | Temp (°C) | Measured thickness (µm) | | | Alteration rate (µm yr^{-1}) |
				Min	Max	Average	
BB1b	Natural	1500 years[b]	5.4	0.5	62	16	0.04
BA5 – 1250	PCT[a]	7 days	90	NA	NA	0.043	2.2
BA5 – 1400	PCT	7 days	90	NA	NA	0.033	1.7
BA5 - Lab oxides	PCT	7 days	90	NA	NA	0.036	1.9
443-Granite – 1250	PCT	7 days	90	NA	NA	0.039	2.0
443-Granite – 1400	PCT	7 days	90	NA	NA	0.028	1.5
443-Granite - Lab oxides	PCT	7 days	90	NA	NA	0.089	4.6
BA5 – 1250 (Na at pH 8.9)	EPA 1313	2 days	22	NA	NA	0.009	0.49
BA5 – 1250 (Si at pH 8.9)	EPA 1313	2 days	22	NA	NA	0.004	0.19
BA5 – 1250	VHT	24 days	200	2	4	3	61
BA5 – 1400	VHT	24 days	200	NM	NM	NM	0
BA5 - Lab oxides	VHT	24 days	200	NM	NM	NM	0
443-Granite – 1250	VHT	24 days	200	NM	NM	NM	0
443-Granite – 1400	VHT	24 days	200	1	30	11	456
443-Granite - Lab oxides	VHT	24 days	200	NM	NM	NM	0
Dike amphibolite	VHT	49 days	200	4	40	10	298
BA5 – 1250	VHT	49 days	200	2	45	11	335
BB1b	VHT	49 days	200	0.1	13	1.8	96

The alteration rate is based on the thickest measurement as a means of conservatism.
NA not available, NM non-measurable.
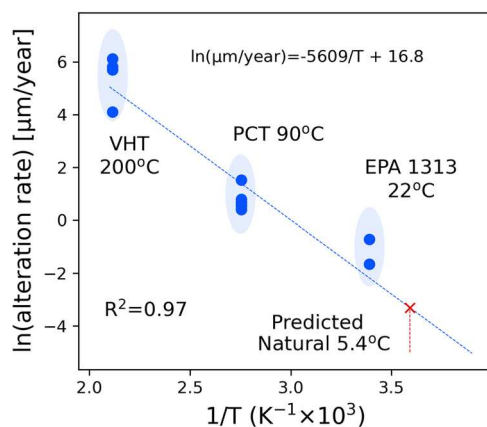[a]All PCT thicknesses are calculated from Na results.

Fig. 10 An Arrhenius plot showing the natural log of the estimated alteration rate (µm yr^{-1}) as a function of the inverse temperature (K^{-1}). The linear relationship between the tests suggests that the rate-controlling mechanisms of corrosion might be similar in the different cases.

from laboratory tests to reaction rates from site samples. The linear relationship between the laboratory and environmentally altered samples suggests that the rate-controlling mechanisms of corrosion might be similar, despite the very different environmental conditions and reaction regimes. However, it remains to be confirmed that the mineral phases produced by environmental alteration mechanisms can be reproduced in the laboratory. In addition, there are other environmental variables, including microbial activity, porewater pH, temperature, and the cycling between wet and dry conditions, that can influence the corrosion rate of the vitrified material. These environmental parameters are not accounted for in standard accelerated tests. Alternative tests,

such as EPA LEAF methods are under investigation to evaluate if the integrated results can holistically provide a direct link to glass waste form performance under the specific conditions of the disposal environment.

METHODS

Melting experiments

The BA5 and Dike amphibolite rocks and the 443 Granite rock samples (Fig. 1) were melted individually in the furnace at different temperatures (1250, 1300 and 1400 °C). Between each melt, the samples were quenched by pouring onto a stainless-steel plate to cool. When a second melt was performed, the sample was ground to a fine powder in a tungsten carbide milling chamber before remelting. Both BA5 amphibolite and the 443 Granite were heterogenous (i.e., there was a remaining crystal fraction as observed visually) after a 1 h melt in a crucible (platinum with 10 wt % rhodium) at a temperature of 1250 °C, which is close to the maximum temperature that has been postulated to have been used for the Broborg vitrification process[25]. Melting the BA5 amphibolite for 1 h at 1250 °C formed samples with characteristics similar to the Broborg archeological glass sample (BB1b). More specifically, the glass sample contained numerous µm-sized iron-containing crystals and small rounded grains of unmelted quartz. The 443 Granite remained largely unmelted at 1250 °C. Production of a homogeneous sample from the 443 Granite and BA5 amphibolite samples required two melts (Table 2). A homogeneous sample with no unmelted quartz was produced with the Dike amphibolite sample after only one melt for ~80 min at 1300 °C.

Lab-made samples with the chemical compositions similar to that for the BA5 amphibolite and 443 Granite were also prepared from laboratory oxide chemicals melted twice for 1 h at 1400/1450 °C, with grinding to a fine powder between melts. A comparison of the samples produced from one of the amphibolites (BA5) and 443 Granite, along with these lab-made samples, allowed for the influence of mineralogy on melting and alteration behavior to be assessed.

Chemical analysis of materials

The bulk chemical compositions of the BA5 amphibolite and granite rock samples from Broborg analyzed and averaged to address possible bulk

compositional heterogeneity (Table 1). Boron was measured with a closed system vessel digestion using concentrated nitric, hydrochloric and hydrofluoric acids. Aluminum, calcium, chromium, iron, silicon, titanium and zirconium were measured with a lithium metaborate/tetraborate fusion. Remaining metals were measured by digesting the solids in concentrated nitric, perchloric, hydrofluoric and hydrochloric acids in an open vessel. The resulting digestates were analyzed by ICP-OES.

Composition of the Dike sample was measured using a JEOL 8530 F electron probe microanalyzer operated at 15KV accelerating voltage and 20 nA probe current. Linear time-dependent intensity corrections were performed for sodium drift, for further experimental details see McCloy et al. [26] Composition of the lab-made granite was checked using a JEOL 7001 scanning electron microscope using energy-dispersive spectroscopy (EDS).

Sample preparation

The samples produced as a result of these melting experiments were prepared in two different physical forms: annealed monoliths for VHT and as-quenched samples ground into powder for PCT and EPA Method 1313 (LAWA44 was only prepared as a powder for EPA 1313). The annealing process consisted of pouring the molten material into a stainless-steel mold, allowing the sample to cool until it was solid to the touch of a stainless-steel spatula, and then transferring to an oven at 515 °C. The sample was held at 515 °C for 1 h and slow cooled to room temperature overnight in the oven. The annealed bars were cut using a Buehler low-speed Isomet saw equipped with a diamond blade to form ~1 × 1 × 0.15 cm coupons. In accordance with ASTM C1663[22], the coupons were then polished with SiC abrasive grinding paper of increasing fineness, starting with 240 and ending with 600 grit. For PCTs, a quenched sample was formed by pouring the molten material onto an Inconel® plate, which cooled the glass to room temperature in several minutes. This quenched material was crushed using a tungsten carbide grinding chamber and sieved with stainless-steel sieves to obtain 75–150 μm glass particles. In accordance with ASTM C1285[21], the particles were ultrasonically washed with water and then ethanol to remove fines adhering to the surface.

Sectioning of post-reaction solids was necessary to produce samples suitable for SEM-EDS analysis. A dry Isomet slow speed saw (Buehler) was used to subsection VHT samples for SEM. Samples were prepared for SEM by first mounting in epoxy and then polishing with diamond paste and non-aqueous lubricants, including colloidal silica. Polishing was performed on a lapidary wheel until the surface roughness was ≈1–10 μm, then on a vibratory polisher to give a final sub-micron surface finish (surface roughness ≈0.02–0.05 μm) suitable for imaging.

Modified product consistency tests

Static corrosion tests were either performed using the PCT-A method or a modified version of the PCT-B method[21]. For the PCT-A method, all tests consisted of adding 1 g of prepared samples into a 22 mL stainless steel vessel, adding 10 mL of deionized water, and placing the vessel in a convection oven at 90 °C for 7 days (±2 h). At the end of the experiment, the leachant solution was analyzed by ICP-OES.

The modified PCT-B tests were started by adding 0.5 g glass powder to ≈50 mL deionized water in a PTFE vessel [(S/V) = 200 m^{-1}]. Vessels were then sealed and heated in a convection oven at 90 °C. The tests are considered modified PCT-B because the vessels were opened, and solution was removed while the test was ongoing. Solution aliquots of 250 μL were taken at specific intervals (3, 7, 14, 28, 42, 62, and 91 days). The aliquots were acidified with 2.75 mL with 0.3 mol L^{-1} HNO$_3$ prior to elemental analysis by ICP OES. Test and solution data are provided in the Table S1.

Acidified solution aliquots were quantitatively analyzed for major element concentrations by ICP OES using a PerkinElmer OptimaTM 8300 dual view instrument with an Elemental Scientific SC4 DX FAST auto-sampler. The pH was also measured regularly at the test temperature directly in the alteration vessel, with a glass pH electrode (AccumetTM) calibrated at test temperature.

The normalized concentration (NC$_i$) values were calculated using the following equation:

$$NC_i = \frac{[X]_i}{f_i} \tag{1}$$

where $[X]_i$ is the concentration of element i (g m^{-3}) and f_i is the normalized concentration of element i in the starting material (unitless). The normalized mass loss (NL$_i$) values were calculated using the following

equation:

$$NL_i = NC_i \cdot \frac{V}{S} \tag{2}$$

where V is the solution volume (m^3) and S is the surface area of the glass (m^2). The NL$_i$ value allows comparison of the relative durability of different materials normalized to the surface area of the material. The NL$_i$ value can then be used to calculate an estimated alteration layer thickness based on element i using:

$$AL_i = \frac{NL_i}{\rho} \tag{3}$$

where AL$_i$ is the estimated alteration layer thickness (m) and ρ is the glass density (g m^{-3}). Equation 3 is best at estimating AL$_i$ when used with a soluble element (e.g., B and Na) and presenting results of AL$_i$ for insoluble elements (e.g., Si and Al) provides an estimate of the relative release of each element into solution.

The experimental uncertainty of NL$_i$ and AL$_i$ can be calculated by considering the uncertainties for each variable in Eqs. (1) and (2). For uncorrelated random errors, the standard deviation of a function of the form $f(x_1, x_2, x_n)$ is estimated using the standard, first-order error propagation method:

$$\sigma_f = \sqrt{\sum_{i=1}^{n} \left(\frac{\delta f}{\delta x_i}\right)^2 \sigma_i^2} \tag{4}$$

where σ_f is standard deviation of the function f, x_i is parameter i, and σ_i is standard deviation of parameter i.

Substitution of Eq. 1 in Eq. 4 and using a relative error, $\hat{\sigma}_{r_i} = \sigma_{r_i}/r_i$, the following equation is obtained:

$$\hat{\sigma}_f = \sqrt{\hat{\sigma}_{X_i}^2 + \hat{\sigma}_{f_i}^2} \tag{5}$$

Substitution of Eq. 2 in Eq. 4 and using a relative error, $\hat{\sigma}_{r_i} = \sigma_{r_i}/r_i$, the following equation is obtained:

$$\hat{\sigma}_f = \sqrt{\hat{\sigma}_{NC_i}^2 + \hat{\sigma}_S^2 + \hat{\sigma}_V^2} \tag{6}$$

Relative errors of 10%, 10%, 15% and 1% are assigned to X_i, f_i, S, and V, respectively. Similarly, the relative uncertainty applied to Eq. 3 results in the following equation.

$$\hat{\sigma}_f = \sqrt{\hat{\sigma}_{NL_i}^2 + \hat{\sigma}_\rho^2} \tag{7}$$

Where the relative error for NL$_i$ is determined from Eq. 4 and the relative uncertainty for ρ is 5%. Equations 4, 5, and 6 result in relative uncertainties of 14%, 21% and 21% for NC$_i$, NL$_i$ and AL$_i$.

Procedure for vapor hydration test (VHT)

Coupons of known dimensions (roughly 1 cm × 1 cm × 0.1 cm) were suspended from a stainless-steel support rod inside the vessel with platinum wire (e.g., Figure 10a), and deionized water (0.25 mL) was added. The vessel was then sealed, tightened with a torque wrench to avoid vapor loss, and held at 200 °C in an oven for 24 or 49 days. After the test, the vessel was removed from the oven and cooled in water to condense the vapor in the vessel. Coupons were removed, prepared as explained above, and examined with optical microscopy and SEM to measure an alteration thickness.

US EPA method 1313 procedure

For each of the nine batch extractions, 1 g of particles, with a size of 75–150 μm were contacted with leaching solution at a liquid-to-solid ratio of 10 mL g^{-1} and tumbled end-over-end for a 48 ± 2 h contact interval at room temperature (~22 °C). The leaching solution was reagent water with additions of nitric acid (HNO$_3$) or potassium hydroxide (KOH) to target the final pH of the eluate to nine specific pH values (i.e., 2, 4, 5.5, 7, 8, 9, 10.5, 12, and 13). An additional extraction in reagent grade water without addition of acid or base was carried out to measure constituent leaching at the natural pH of the material. The sample aliquot from the test was measured for pH and electrical conductivity (EC). The remaining solution from the test was syringe-filtered through 0.45 μm pore size membranes and then acidified with 1% v/v nitric acid prior to chemical analysis by ICP-MS and ICP-OES. Further details of application of the EPA 1313 test to glass samples is provided elsewhere[49]. A plot of the EPA 1313 concentration

data is provided in Supplementary Fig. 5. Test and solution data are provided in the Supplementary Table 2 and Supplementary Table 3.

Scanning electron microscopy (SEM)

Samples were analyzed with a JEOL JSM 7001 F field emission gun SEM. SEM conditions of 15 kV accelerating voltage, 13 nA probe current, aperture size 4, and a 10 mm working distance were used. A short working distance backscatter detector (BSE) was used to capture the signal for micrograph collection. Energy-dispersive X-ray spectroscopy (EDS) was performed on select samples and that information is provided in the (Supplementary Fig. 2).

Geochemical calculations

The Geochemists Workbench 12.0 software[50] was used to calculate saturation indices with the use of the LLNL thermodynamic dataset[51].

DATA AVAILABILITY

The datasets generated and analyzed during the current study are available from the corresponding author on reasonable request, included in this article, or in the Supplementary Information.

REFERENCES

1. Weaver, J. L. et al. Pre-viking Swedish hillfort glass: a prospective long-term alteration analogue for vitrified nuclear waste. *Int. J. Appl. Glass Sci.* **9**, 540–554 (2018).
2. Libourel, G. et al. The use of natural and archeological analogues for understanding the long-term behavior of nuclear glasses. *C. R. Geosci.* **343**, 237–245 (2011).
3. Ewing, R. C. & Roed, G. Natural analogues: their application to the prediction of the long-term behavior of nuclear waste glasses. *Mater. Res. Soc. Symp. Proc.* **84**, 67–83 (1987).
4. Ewing, R. C. Natural glasses: analogues for radioactive waste forms. *Mater. Res. Soc. Symp. Proc.* **1**, 57–68 (1979).
5. Ahmadzadeh, M., García-Lasanta, C., Housen, B. & McCloy, J. S. Archaeomagnetic dating of vitrified Broborg hillfort in southeast Uppsala, Sweden. *J. Archaeol. Sci. Rep.* **31**, 102311 (2020).
6. Plymale, A. E. et al. Niche Partitioning of Microbial Communities at an Ancient Vitrified Hillfort: Implications for Vitrified Radioactive Waste Disposal. *Geomicrobiol. J.* **38**, 1–21 (2020).
7. Michelin, A. et al. Effect of iron metal and siderite on the durability of simulated archeological glassy material. *Corros. Sci.* **76**, 403–414 (2013).
8. Verney-Carron, A., Gin, S. & Libourel, G. Archaeological analogs and the future of nuclear waste glass. *J. Nucl. Mater.* **406**, 365–370 (2010).
9. Majérus, O. et al. Glass alteration in atmospheric conditions: crossing perspectives from cultural heritage, glass industry, and nuclear waste management. *npj Mater. Degrad.* **4**, 27 (2020).
10. Palomar, T., Silva, M., Vilarigues, M., Pombo Cardosos, I. & Giovannacci, D. Impact of solar radiation and environmental temperature on Art Nouveau glass windows. *Herit. Sci.* **7**, 82 (2019).
11. Rodrigues, A., Fearn, S., Palomar, T. & Vilarigues, M. Early stages of surface alteration of soda-rich-silicate glasses in the museum environment. *Corros. Sci.* **143**, 362–375 (2018).
12. Morgenstein, M. E. & Shettel, D. L. Volcanic Glass as a Natural Analog for Borosilicate Waste Glass. *Mater. Res. Soc. Symp. Proc.* **333**, 605–615 (1993).
13. Crovisier, J.-L., Advocat, T. & Dussossoy, J.-L. Nature and role of natural alteration gels formed on the surface of ancient volcanic glasses (Natural analogs of waste containment glasses). *J. Nucl. Mater.* **321**, 91–109 (2003).
14. Crovisier, J.-L., Advocat, T., Petit, J. C. & Fritz, B. Alteration of Basaltic Glass in Iceland as a Natural Analogue for Nuclear Waste Glasses: Geochemical Modelling with DISSOL. *Mater. Res. Soc. Symp. Proc.* **127**, 57–64 (1989).
15. Sessegolo, L. et al. Long-term weathering rate of stained-glass windows using H and O isotopes. *npj Mater. Degrad.* **2**, 17 (2018).
16. Palomar, T. & Llorente, I. Decay processes of silicate glasses in river and marine aquatic environments. *J. Non-Cryst. Solids* **449**, 20–28 (2016).
17. Jantzen, C. M., Brown, K. G. & Pickett, J. B. Durable glass for thousands of years. *Int. J. Appl. Glass Sci.* **1**, 38–62 (2010).

18. Grambow, B. Nuclear waste glasses - How durable? *Elements* **2**, 357–364 (2006).
19. Englund, M. *Broborg Hillfort: A Research Study of the Vitrified Wall, Report 2018:103* (The Archaelogists. The National Historical Museums, Stockholm, Sweden, 2018).
20. Ogenhall, E. *Amphibolitic Rocks Near Broborg, Uppland. GAL PM 2016:03* (The Archaelogists. The National Historical Museums, Stockholm, Sweden, 2018)
21. ASTM C1285-21, *Standard Test Methods for Determining Chemical Durability of Nuclear, Hazardous, and Mixed Waste Glasses and Multiphase Glass Ceramics: The Product Consistency Test (PCT).* (ASTM International, West Conshohocken, PA, 2021).
22. ASTM. C1663-18, *Standard Test Method for Measuring Waste Glass or Glass Ceramic Durability by Vapor Hydration Test.* (ASTM International, West Conshohocken, PA, 2018).
23. U. S. EPA, Method 1313, *Liquid-solid Partitioning as a Function of Extract pH using a Parallel Batch Extraction Procedure.* (Environmental Protection Agency, SW-846 Update VII, Revison 1, Washington, DC, 2019).
24. Kresten, P. & Ambrosiani, B. Swedish vitrified forts–a reconnaissance study. *Fornvännen J. Swed. Antiqu. Res.* **87**, 1–17 (1992).
25. Sjöblom, R. et al. Vitrified hillforts as anthropogenic analogues for nuclear waste glasses – project planning and initiation. *Int. J. Sustain. Dev. Plan.* **11**, 897–906 (2016).
26. McCloy, J. S. et al. Reproduction of melting behavior for vitrified hillforts based on amphibolite, granite, and basalt lithologies. *Sci. Rep.* **11**, 1272 (2021).
27. Matthews, B., Arey, B., Pearce, C. & Kruger, A. Characterization of Glass Alterations in Ancient Glass from Various Environments from Broborg, a Vitrified Swedish Hillfort. *Microsc. Microanal.* **26**, 2592–2593 (2020).
28. Gin, S., Ryan, J. V., Schreiber, D. K., Neeway, J. J. & Cabié Contribution of atom-probe tomography to a better understanding of glass alteration mechanisms: application to a nuclear glass specimen altered 25 years in a granitic environment. *Chem. Geol.* **349-350**, 99–109 (2013).
29. Jantzen, C. M., Bibler, N. E., Beam, D. C., Crawford, C. L., Pickett, J. B. *Characterization of the Defense Waste Processing Facility (DWPF) Environmental Assessment (EA) Glass Standard Reference Material.* WSRC-TR-92-346, Rev. 1. (Westinghouse Savannah River Co., Aiken, SC, 1993).
30. U.S. DOE. *Waste Acceptance Product Specifications for Vitrified High-Level Waste Forms (WAPS).* DOE/EM-0093, U.S. (Department of Energy, Office of Environmental Management, Washington, DC,1996).
31. U.S. DOE. *Design, Construction, and Commissioning of the Hanford Tank Waste Treatment and Immobilization Plant. Contract DE-AC27-01RV14136, as Amended, U.S.* (Department of Energy, Office of Civilian Waste Management, Richland, WA, 2000).
32. Jiřička, A., Vienna, J. D., Hrma, P. & Strachan, D. M. The effect of experimental conditions and evaluation techniques on the alteration of low activity glasses by vapor hydration. *J. Non-Cryst. Solids* **292**, 25–43 (2001).
33. Luo, J. S., Ebert, W. G., Mazer, J. J. & Bates, J. K. Simulation of Natural Corrosion by Vapor Hydration Test: Seven-Year Results. *Mater. Res. Soc. Symp. Proc.* **465**, 157–163 (1996).
34. Neeway, J. et al. Vapor hydration of SON68 glass from 90 °C to 200 °C: A kinetic study and corrosion products investigation. *J. Non-Cryst. Solids* **358**, 2894–2905 (2012).
35. Fournier, M., Gin, S. & Frugier, P. Resumption of nuclear glass alteration: State of the art. *J. Nucl. Mater.* **448**, 348–363 (2014).
36. Pierce, E. M. et al. *Waste Form Release Data Package for the 2005 Integrated Disposal Facility Performance Assessment.* Report No. PNNL-14805, (Pacific Northwest National Laboratory, Richland, WA, 2004).
37. Inagaki, Y., Kikunaga, T., Idemitsu, K. & Arima, T. Initial dissolution rate of the International Simple Glass as a function of pH and temperature measured using Microchannel Flow-Through Test method. *Int. J. Appl. Glass Sci.* **4**, 317–327 (2013).
38. Strachan, D. Glass dissolution as a function of pH and its implications for understanding mechanisms and future experiments. *Geochim. Cosmochim. Acta* **219**, 111–123 (2017).
39. Verney-Carron, A., Gin, S. & Librourel, G. A fractured roman glass block altered for 1800 years in seawater: Analogy with nuclear waste glass in a deep geological repository. *Geochim. Cosmochim. Acta* **72**, 5372–5385 (2008).
40. Verney-Carron, A., Gin, S., Frugier, P. & Libourel, G. Long-term modeling of alteration-transport coupling: application to a fractured Roman glass. *Geochim. Cosmochim. Acta* **74**, 2291–2315 (2010).
41. Lombardo, T. et al. Characterisation of complex alteration layers in medieval glasses. *Corros. Sci.* **72**, 10–19 (2013).
42. Kim, D. S., Peeler, D. K. & Hrma, P. Effects of crystallization of hte chemical durability fo nuclear waste glasses. *Ceram. Trans.* **61**, 177–185 (1995).
43. Vienna, J. D. et al. *2016 Update of Hanford Glass Property Models and Constraints for Use in Estimating the Glass Mass to be Produced at Hanford by Implementing Current Enhanced Glass Formulation Efforts.* PNNL-25835. (Pacific Northwest National Laboratory, Richland, WA, 2016).
44. Aréna, H., Rébiscou, D., Garcès, E. & Godon, N. Comparative effect of alkaline elements and calcium on alteration of International Simple Glass. *npj Mater. Degrad.* **3**, 10 (2019).

45. Aréna, H. et al. Impact of Fe, Mg and Ca elements on glass alteration: interconnected processes. *Geochim. Cosmochim. Acta* **239**, 420–445 (2018).
46. Fleury, B., Godon, N., Ayral, A. & Gin, S. SON68 glass dissolution driven by magnesium silicate precipitation. *J. Nucl. Mater.* **442**, 17–28 (2013).
47. Jantzen, C. M. & Bickford, D. F. Leaching of Devitrified Glass Containing Simulated SRP Nuclear Waste. *Mater. Res. Soc. Symp. Proc.* **44**, 135–146 (1985).
48. Neeway, J. J., Rieke, P. C., Parruzot, B. P., Ryan, J. V. & Asmussen, R. M. The dissolution behavior of borosilicate glasses in far-from equilibrium conditions. *Geochim. Cosmochim. Acta* **226**, 132–148 (2018).
49. Marcial, J. et al. Evaluating an EPA leaching test (Method 1313) to relate the long-term performance of nuclear waste glasses and ancient glasses - 21243 WM2021 Conference, Phoenix, Arizona, USA (2021).
50. Bethke, C. M. *Geochemical Reaction Modeling*. 2nd edn. (Oxford University Press, 2008).
51. Wolery, T. J. *EQ3NR, a computer program for geochemical aqueous speciation-solubility calculations: Theoretical manual, user's guide, and related documentation (Version 7.0)*; Part 3. UCRL-MA-110662. (Lawrence Livermore National Laboratory, Livermore, CA, 1992).

AUTHOR CONTRIBUTIONS

L.N-F. performed experiments, analyzed data and contributed to the writing of the paper. J.J.N. designed experiments, analyzed data and contributed to the writing of the paper. M.J.S. designed experiments, analyzed data and contributed to the writing of the paper. J.M. performed experiments, analyzed data and contributed to the writing of the paper. N.L.C. performed microscopy on altered samples. C.I.P. discussed and contributed to the writing of the paper. D.K.P. contributed to the writing of the paper. E.P.V. performed microscopy and quantitative analysis on samples before alteration. D.S.K. discussed and contributed to the writing of the paper. R.C.D. performed solution analysis. J.S.M. discussed and contributed to the writing of the paper. S.A.W. performed experiments. C.L.T. discussed and contributed to the writing of the paper. C.L.C. discussed and contributed to the writing of the paper. R.J.H. discussed and contributed to the writing of the paper. R.S. discussed and contributed to the writing of the paper. A.A.K. discussed and contributed to the writing of the paper.

COMPETING INTERESTS

The authors declare no competing interests.

ADDITIONAL INFORMATION

Supplementary information The online version contains supplementary material available at https://doi.org/10.1038/s41529-021-00204-2.

Correspondence and requests for materials should be addressed to James J. Neeway.

Reprints and permission information is available at http://www.nature.com/reprints

Publisher's note Springer Nature remains neutral with regard to jurisdictional claims in published maps and institutional affiliations.